TU/e EINDHOVEN UNIVERSITY OF TECHNOLOGY

Quantum chemistry of surface chemical reactivity

Citation for published version (APA):
van Santen, R. A. (1991). Quantum chemistry of surface chemical reactivity. In H. H. Brongersma, & R. A. van Santen (Eds.), *Fundamental aspects of heterogeneous catalysis studied by particle beams : NATO advanced study institute, held September 3-14, 1990, Alicante, Spain* (pp. 83-111). (NATO ASI Series, Series B: Physics; Vol. 265). Plenum Press. https://doi.org/10.1007/978-1-4684-5964-7_9

DOI:
10.1007/978-1-4684-5964-7_9

Document status and date:
Published: 01/01/1991

Document Version:
Publisher's PDF, also known as Version of Record (includes final page, issue and volume numbers)

Please check the document version of this publication:

• A submitted manuscript is the version of the article upon submission and before peer-review. There can be important differences between the submitted version and the official published version of record. People interested in the research are advised to contact the author for the final version of the publication, or visit the DOI to the publisher's website.
• The final author version and the galley proof are versions of the publication after peer review.
• The final published version features the final layout of the paper including the volume, issue and page numbers.

Link to publication

General rights
Copyright and moral rights for the publications made accessible in the public portal are retained by the authors and/or other copyright owners and it is a condition of accessing publications that users recognise and abide by the legal requirements associated with these rights.

• Users may download and print one copy of any publication from the public portal for the purpose of private study or research.
• You may not further distribute the material or use it for any profit-making activity or commercial gain
• You may freely distribute the URL identifying the publication in the public portal.

If the publication is distributed under the terms of Article 25fa of the Dutch Copyright Act, indicated by the "Taverne" license above, please follow below link for the End User Agreement:

www.tue.nl/taverne

Take down policy
If you believe that this document breaches copyright please contact us at:

openaccess@tue.nl

providing details and we will investigate your claim.

Download date: 04. Oct. 2023

QUANTUM CHEMISTRY OF SURFACE CHEMICAL REACTIVITY

R.A. van Santen

Schuit Institute of Catalysis
University of Technology
P.O. Box 513
5600 MB EINDHOVEN
The Netherlands

Abstract

The quantum chemist's and surface physicist's view of the surface chemical bond are illustrated by means of chemisorption of CO as an example. Between adsorbate and metal surface bonding as well as antibonding orbital fragments are formed. For molecules the adsorption geometry is a sensitive function of the balance of the repulsive atop directing interaction, resulting from the occupation of antibonding orbital fragments, and the high coordination directing bonding interaction. The bonding contribution to the surface chemical bond energy relates to the surface group orbital local density of states around the Fermi level, as long as the orbital interactions are weak. The concepts of Pauli repulsion and group orbital LDOS can be used to provide a quantum-chemical basis to metal promotion.

Introduction

In recent years theoretical understanding of the surface chemical bond has significantly increased. Whereas a decade ago the quantum chemistry of organic molecule reactivity and also of organometallic chemistry had reached a more advanced level that that of surface reactivity this knowledge gap is rapidly closing. This is not only the result of the increasing interest of quantum chemists for problems on surface reactivity, but also due to the wealth of rich and detailed molecular and electronic information provided for by experimental surface scientific researchers. Two developments are important from a quantum-chemical point of view.The availability of semi-empirical methods resulting in a conceptual framework to analyse quantum-chemical calculations. Secondly the possibility to use first principle theoretical techniques as the local density approximation as well as other highly sophisticated ab-initio methods in the study of adsorption models of direct interest to the surface chemist. The aim of this paper is to present the essential

Fundamental Aspects of Heterogeneous Catalysis Studied by Particle Beams,
Edited by H.H. Brongersma and R.A. van Santen, Plenum Press, New York, 1991

features of the electronic basis of surface chemical reactivity. The theoretical-chemical application of surface chemical bonding theory that we will highlight is related to formal chemisorption theory as developped in surface physics, but focusses rather on typical quantum-chemical concepts as the electron occupation of bonding and antibonding orbital fragments than on properties as the local density of states or surface states well known to the surface physicist. We will see that both approaches complement each other. The local density of states concept stemming from surface physics is also indispensable to the surface chemist. The idea of a surface molecule relates to the surface physicists concept of surface states.

We will start with a quantum chemists view of chemisorption of CO to a transition metal surfaces. The surface chemical bond of CO is theoretically as well as experimentally very well understood. Of extreme importance has been Blyholder's (1) view of the surface chemical bond. It is analogous to the Frontier Orbital (2) concept widely used by chemists. Bonding is considered to be the result of the interaction of Highest Occupied Molecular (HOMO) Orbitals in one of the interacting fragments and the Lowest Unoccupied Molecular Orbitals (LUMO) on the other fragment and visa versa. On a surface this results in a sum of two terms. A contribution due to the interaction between occupied adsorbate orbitals and empty metalsurface orbitals (donation) and a second contribution due to the interaction of occupied metal surface orbitals and empty adsorbate orbitals (backdonation). Whereas this provides a satisfactory description for the attractive part of the interaction potential, it does not provide a prescription to estimate the repulsive part of the interaction potential. The coordination of molecules to surfaces cannot be understood without a proper understanding of the latter. More recent developments, mainly based on extension of the Extended-Hückel method but verified with first principle calculations, provide a consistent view of the surface chemical bond incorporating Pauli repulsion, useful to the surface chemical theorist (3). This leads to a significant modification of the original Blyholder approach. In the next section the theoretical basis will be presented and applied to a few other examples in the final section. In the third section the Newns-Anderson (4) approach to chemisorption will be introduced. This represents the surface physicist's approach to the surface chemical bond.

The framework provided for by formal chemisorption theory can be readily shown to be very similar to the theoretical chemical ideas discussed above. It will appear that chemisorption of molecules to transition metals has to be considered intermediate between the so-called weak adsorption and surface molecule strong adsorption limits, As in chemical bonding theory also formal chemisorption theory can be shown to be consistent with the formation of bonding as well as antibonding adsorbate-surface fragment orbitals.The electron occupation of these bonding and antibonding fragment orbitals determines the adsorbate-surface bond strength. The broadening of the adsorbate orbitals will be found to relate to the local density of states of the metal surface orbitals close to the maximum of the adsorbate orbital density. Extending HOMO-LUMO theory to metalsurfaces local density of states around the Fermi level (5), the theoretical results of this section will be illustrated by a discussion of O_2 chemisorption to the silversurface (6) and the CO bond strength on different transition metalsurfaces (7).
In the final section the concepts presented in the earlier two sections are applied to changes in chemical reactivity due to coadsorption of promoters. It will appear that some promoters change the attractive part of the interaction potential, whereas others reduce Pauli repulsion, that contributes to the repulsive part of the adsorbate-surface interaction potential. This will be illustrated by discussing the changes in CO chemisorption to a metal surface or metalparticles due to the presence of coadsorbed cations. It also provides an opportunity to discuss the importance of local electrostatic effects and

polarization to the surface chemical bond. Coadsorption of sulfur primarily effects the attractive part of the interaction energy. Finally the electronic basis of the promoting action of coadsorbed subsurface oxygen or chloride on the ethylene epoxidation rate catalysed by silver will be discussed (8). In this example the coadsorbate changes a repulsive interaction into an attractive one.

Molecular orbital theory of CO chemisorption

The interaction between the molecular orbitals of CO and those of the surface will lead to new molecular orbitals, that can be decomposed into bonding and antibonding orbitals with respect to the originally undisturbed fragment orbitals. In quantum chemistry the bonding or antibonding nature of orbital fragments is deduced from the bond-order overlap population density. Let the free adsorbate orbitals be given by φ_i and the metalsurface orbitals be given by ϕ_k, then the molecular orbitals Ψ_λ of the interacting system can be written as:

$$\Psi_\lambda = \sum_i c_i^\lambda \varphi_i + \sum_k c_k^\lambda \phi_k \tag{1a}$$

$$= \sum_i c_i^\lambda \varphi_i + \sum_{k,j} c_k^\lambda d_j^k \chi_j^m \tag{1b}$$

$$= \sum_i c_i^\lambda \varphi_i + \sum_j c_j^{-\lambda} \chi_j^m \tag{1c}$$

Orbitals χ_j^m are the atomic orbitals localized on the metal atoms. It has been assumed that a metalorbital can be written as a linear combination of metal atomic orbitals. In the case of a transition metal elementary molecular orbital theory would choose the metalvalence d-, s- and p-atomic orbitals to form the basisset from which the metal orbitals are composed. Of interest are the bond-order overlap population densities (BOOPD) between adsorbate molecular orbitals φ_i and surface metal atomic orbitals on the surface metal atoms that coordinate with the adsorbate:

$$\pi_{ij}(E) = Re \sum_\lambda c_i^{\lambda^*} c_j^\lambda S_{ij} \, \delta(E - E_\lambda) \tag{2a}$$

$$\text{with :} \quad S_{ij} = \langle \varphi_i \,|\, \chi_j^m \rangle \tag{2b}$$

S_{ij} is the overlap of an adsorbate orbital with a surface metal atomic orbital. Figures 1 and 2 show π_{ij}'s computed according to the Extended Hückel method for a CO molecule atop adsorbed to a 29 atom cluster of Rh atoms simulating the Rh (111) surface. For details we refer to (7). Figures 1 present the BOOPD $\pi_{5\sigma,d_{z^2}}$, $\pi_{5\sigma,s}$ and $\pi_{5\sigma,p}$. These are the only non-zero BOOPD's of s symmetry. Figures 2 present the corresponding non-zero type BOOPD's, $\pi_{2\pi^*,d_{xz}}$. In CO the 5σ orbital, pointing away from the carbon atom to the surface atom is the CO HOMO. The two degenerate $2\pi^*$ orbitals are the CO LUMO's. In the figures E_F denotes the position of the HOMO of the combined CO, cluster system. One notes that at low energies the values of π_{ij} are always positive, but may become negative if the energy increases. The covalent contribution to the bond energy has the form:

$$E_{cov} = 2 \sum_k N_k \sum_{i<j} Re \, c_i^{k^*} c_j^k H_{ij} \tag{3}$$

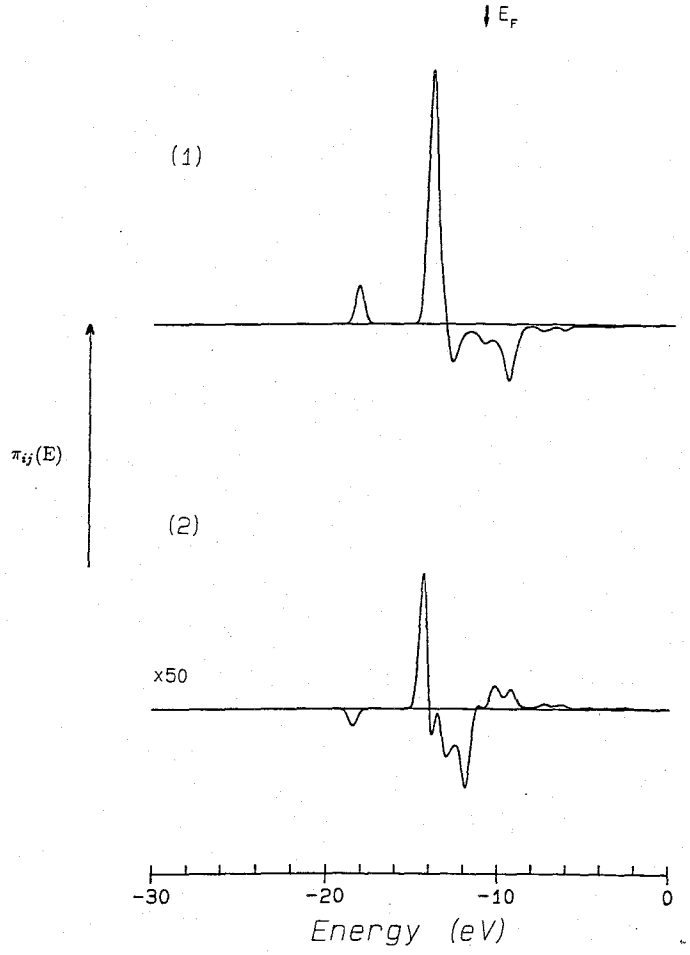

Figure 1a

σ-symmetry bond-order overlap population densities of atop coordinated CO with surface metal orbital on Rh (111), $\pi_{5\sigma,d_z}$.

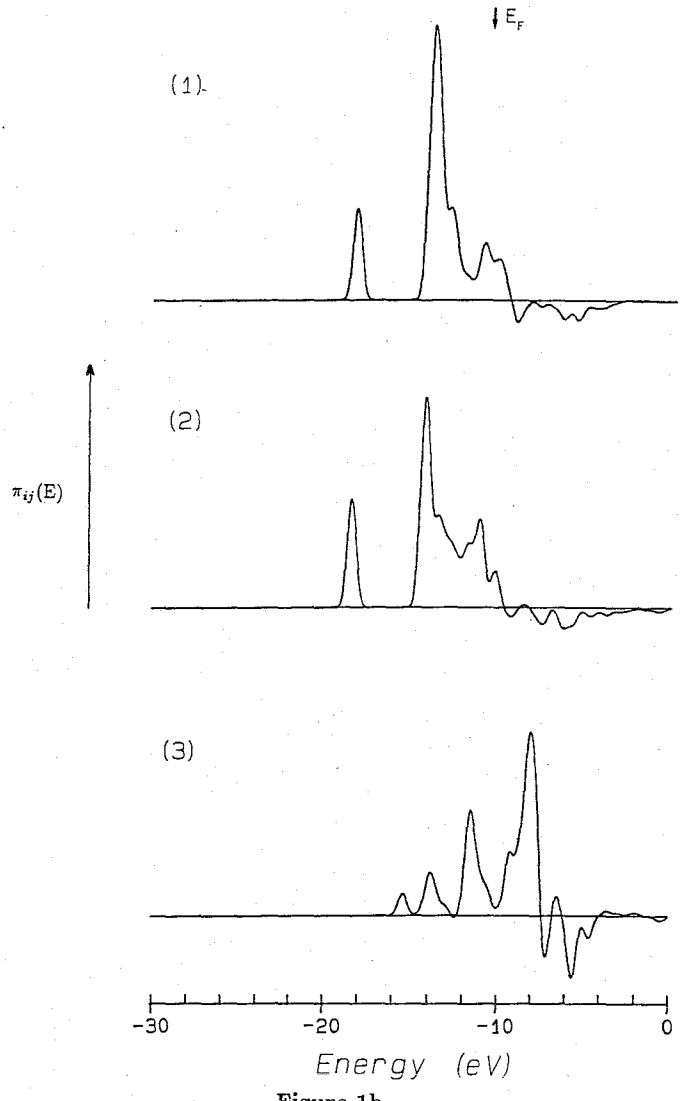

Figure 1b

σ-symmetry bond-order overlap population densities of atop coordinated CO with surface metal orbital on Rh (111), $\pi_{5\sigma,s}$.

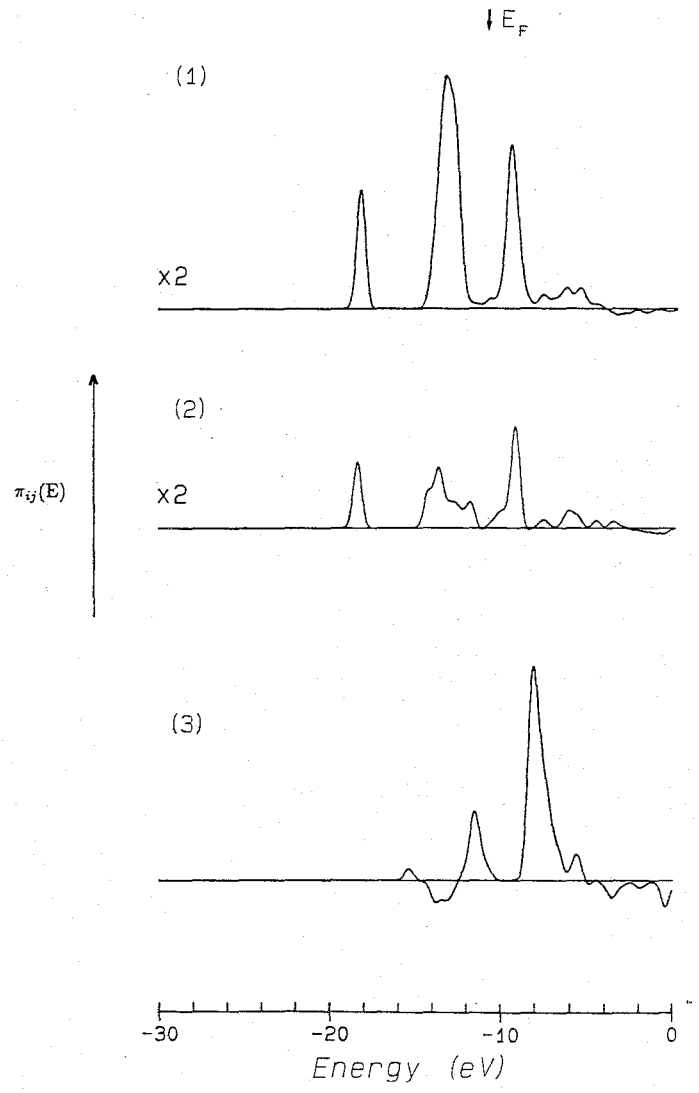

Figure 1c

σ-symmetry bond-order overlap population densities of atop coordinated CO with surface metal orbital on Rh (111), $\pi_{5\sigma,p_z}$.

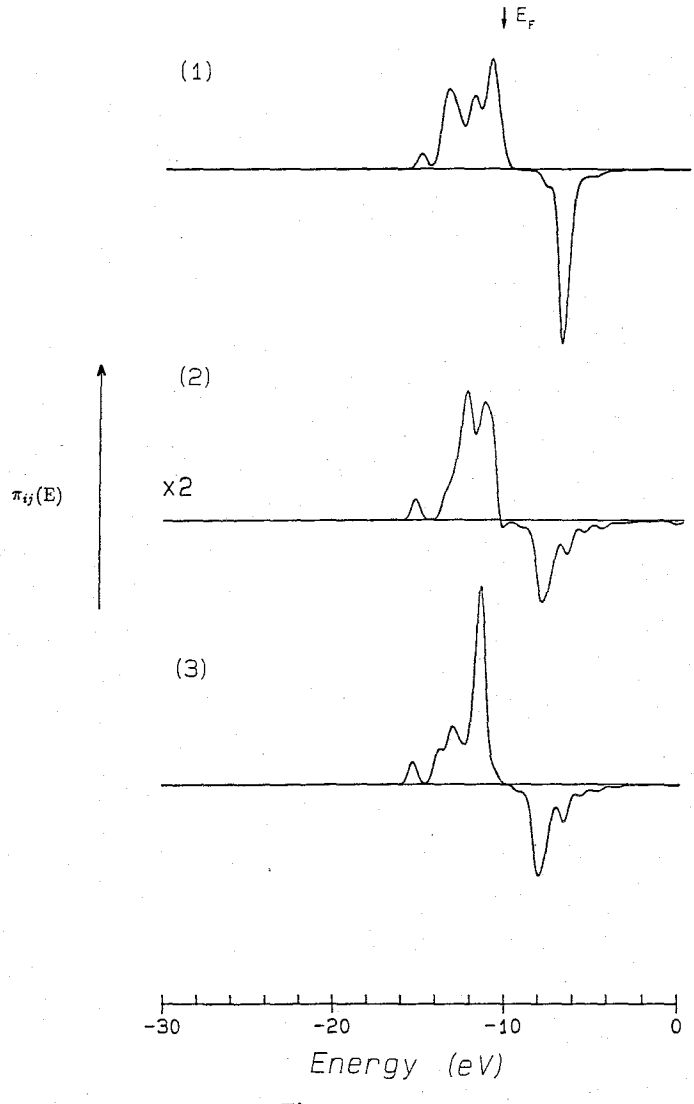

Figure 2

$2\pi^* - d_{xz}$ bond-order overlap population density of atop coordinated CO with d_{xz} metal orbital on Rh (111).

Table 1a. Surface atomic orbital gross populations: 1-fold adsorption of CO on Rh(111).

		1-fold		
	orbital	(111)	(100)	(110)
before adsorption	s	0.293	0.266	0.301
after adsorption		0.518	0.498	0.529
before adsorption	p_x	0.162	0.134	0.102
after adsorption		0.176	0.151	0.127
before adsorption	p_z	0.113	0.111	0.096
after adsorption		0.383	0.387	0.400
before adsorption	$d_{x^2-y^2}$	0.802	0.825	0.854
after adsorption		0.802	0.825	0.862
before adsorption	d_{z^2}	0.922	0.911	0.875
after adsorption		0.667	0.649	0.676
before adsorption	d_{xz}	0.891	0.843	0.923
after adsorption		0.890	0.852	0.909

N_k is the electron occupancy of orbital k and H_{ij} the non-diagonal matrix element of the interaction Hamiltonian. Because of the approximate relationship:

$$H_{ij} \sim S_{ij} \tag{4}$$

a positive value of $\pi_{ij}(E)$ corresponds to a bonding contribution to the bond strength and a negative value of $\pi_{ij}(E)$ an antibonding bond weakening contribution. Note that only for the $5\sigma, d_{z^2}$ interaction antibonding orbital fragments become occupied by electrons. Low lying antibonding orbital fragments are present in $2\pi^*, d_{xz}$ orbital fragments, but they are not occupied. The interaction with s and p valence atomic orbitals is also found to be always bonding.

If the d-valence electron occupation of the transition metal varies the contribution of antibonding $5\sigma, d_{z^2}$ orbital fragments will change. An increase in d-valence electron occupation will weaken the $5\sigma, d_{z^2}$ interaction, a decrease will strengthen it until also bonding orbitals become depopulated. Using metal Rh parameters figure 3 shows that changes of this interaction dominate the computed alteration in bond strength of CO with d-valence electron occupancy. If the Fermi level is chosen such that all antibonding $5\sigma, d_{z^2}$ orbital fragments become occupied, this interaction becomes repulsive. This is for instance the case for the IB metals Cu, Ag and Au. For a spherical symmetric charge distribution this repulsive interaction E_{rep} is proportional to the number of neighbour atoms n (see also 21c):

$$E_{ij}^{rep} \approx n\, S_{ij}^2 \tag{5}$$

Of course depletion of the antibonding orbitalfragments decreases the repulsive interaction and below some orbital occupation it is converted into an attractive interaction. The antibonding orbital fragments of CO coordinated atop deplete more rapidly than the antibonding $5\sigma, d_{z^2}$ orbital fragments formed between CO and metal surface orbitals when chemisorbed in high coordination sites (3). Therefore when the metal d-valence electron occupancy decreases initially the $5\sigma, d_{z^2}$ interaction for CO atop coordinated atop becomes more attractive than that in the higher coordination site.

Table 1b. Surface atomic orbital gross populations: 2-fold adsorption of CO on Rh(111).

		2-fold	
	orbital	σ	π
before adsorption	s	0.327	0.270
after adsorption		0.592	0.317
before adsorption	p_x	0.163	0.167
after adsorption		0.303	0.171
before adsorption	p_y	0.154	0.177
after adsorption		0.171	0.177
before adsorption	p_z	0.115	0.113
after adsorption		0.249	0.173
before adsorption	$d_{x^2-y^2}$	0.939	0.647
after adsorption		0.886	0.643
before adsorption	d_{z^2}	0.940	0.885
after adsorption		0.931	0.870
before adsorption	d_{xy}	0.863	0.720
after adsorption		0.854	0.717
before adsorption	d_{xz}	0.948	0.804
after adsorption		0.787	0.820
before adsorption	d_{yz}	0.900	0.861
after adsorption		0.889	0.857

This changes when the d-valence electron occupation decreases further, when also bonding $5\sigma, d_{z^2}$ orbital fragments become depleted. Then the attractive interaction favouring high coordination-sites starts to dominate. These changes are not easy to verify for d orbitals, because with a change in coordination there is also a large change in the angular dependence of the overlap, so that the interaction with other d atomic orbitals is taken over from that with the d_{z^2} orbitals. This is illustrated in tables 1a and 1b The preference for low coordination when antibonding orbital fragments become initially depleted and the shift to preference of higher coordination with further increase of electron occupancy is due to the fact that in high coordination sites interactions occur with different orbital fragments than in low coordination sites. A σ type orbital will in a high coordination site interact with σ symmetric linear combination of the metal atomic orbitals. This is the group-orbital $\phi_g(n)$, n is the number of surface atoms. When one computes the local density of states ρ_g:

$$\rho_g^{\sigma,m}(E) = \sum_k |\langle \phi_g^{\sigma,m}(n) \mid \phi_k \rangle|^2 \, \delta(E - E_k) \tag{6}$$

one finds that its average electron density shifts to lower energy when n increases (3,9), (see also figure 10). As a consequence at the edge of the electron-density contribution antibonding orbital-fragments have usually a higher density coordinated in the atop position than in higher coordination sites. At lower fragment orbital occupation higher

coordination sites are usually favoured because the bonding orbital fragments have the larger electron density in the bottom of the electron-density contribution in high condination sites.

For symmetric atomic orbital electron densities:

$$H_{ij}^{g} \sim \sqrt{n}\,\beta_{ij}' \tag{7}$$

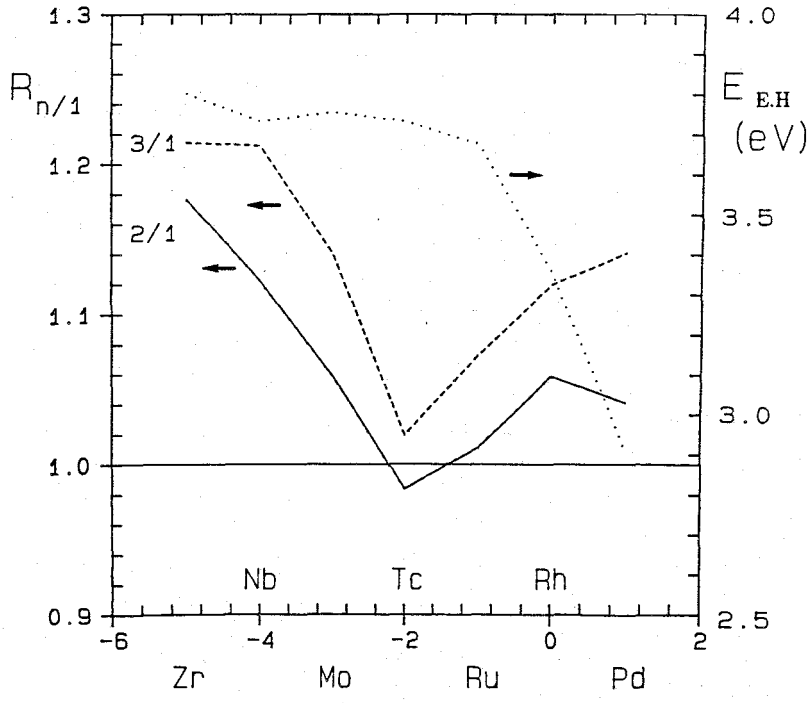

Figure 3

Extended Hückel part of the chemisorptive bond strength ($E_{E.H}$) of atop adsorbed CO on Rh (111) as a function of the occupation of the metal valence electron (dashed line), and the ratio $R_{2/1}$ ($R_{3/2}$) of $E_{E.H}$ of CO adsorbed 2-fold (3-fold) to CO adsorbed on Rh (111) as a function of the occupation of the metal valence electron band (solid line). The elements correspond to the total number of valence electrons according to the periodic system.

H_{ij}^{g} is the interaction Hamiltonian matrix element between adsorbate orbital i and a group orbital consisting of atomic orbitals of type j. β_{ij}' is the corresponding interaction matrix element for atop adsorption. Substition of (7) into (3) results in an additional contribution to covalent stabilization for high coordination sites. The initially decreasing ratio of threefold versus onefold interaction energy of CO shown in fig. 3 with increasing d-valence electron occupation agrees with this analysis. No minimum in this ratio would have been found, if the interaction with the CO $2\pi^*$ orbitals did not change.

As follows from figure 2 only bonding $2\pi^*, d_{xz}$ fragment orbitals are occupied. This usually favours coordination to high coordination sites. In higher coordination sites the $2\pi^*$ will interact with metalsurface group orbitals of π symmetry. Again also an approximate relation as (, is f ..d. ... the interaction with the $2\pi^*$ orbital will not only be attractive for any d-valence electron occupation, but also favours high coordination sites. The minimum in the ratio of threefold versus atop bond energies derives from the decreasing attractive contribution due to orbitals of σ symmetry. With the particular parameters used at high d-valence electron occupation the interaction with orbitals of π symmetry dominates the differences in adsorption site energies. Interestingly CO prefers atop coordination to Rh and Co but higher coordination to Pd and Ni. Apparently on Pd and Ni the interaction with the $2\pi^*$ orbitals dominates. On Pt CO prefers atop adsorption. Because of the higher workfunction of Pt and the large d-orbital extension the balance of the σ and π type interaction remains in favour of the σ-type interaction.

As a result CO prefers atop coordination to a Pt metal surface. As has been shown elsewhere and will discussed shortly in the next section the BOOPD analysis can also be usefully applied to analyse the results of first principle calculations.

Formal chemisorption theory

Chemical bonding theory has to compute BOOPD's and study the occupation of bonding and antibonding orbital fragments to predict adsorption geometries. BOOPD's are experimentally not directly accessible, but useful information to the spectroscopist is provided by the computation of adsorbate orbital local density of states (LDOS), analogous as defined for the metal grouporbitals in (6):

$$\rho_i(E) = \sum_{\lambda} |\langle\varphi_i|\Psi_\lambda\rangle|^2 \, \delta(E - E_\lambda) \tag{8}$$

Note that the group orbital LDOS defined in (6) is calculated by projecting on undisturbed surface metal orbitals, whereas the adsorbate LDOS defined according to (8) is projected on the molecular orbitals of the interacting system.

A major result of formal chemisorption theory (4) is a prediction of the dependence of $\rho_i(E)$ on E:

$$\rho_i(E) = \frac{1}{\pi} \frac{\Gamma_i(E)}{(\alpha_i + \Lambda(E) - E)^2 + \Gamma_i^2(E)} \tag{9a}$$

α_i is the energy of the adsorbate level in the absence of the interaction with the metal surface, $\Lambda_i(E)$ is the level shift function and $\Gamma_i(E)$ the level width function. Explicit expression for $\Lambda_j(E)$ and $\Gamma_i(E)$ are:

$$\Gamma_i(E) = \pi \sum_{k} |\langle\varphi_i|H|\phi_k\rangle|^2 \, \delta(E - E_k) \tag{9b}$$

$$\Lambda_i(E) = \oint dE' \frac{\Gamma_i(E')}{E' - E} \tag{9c}$$

$\oint$ denotes the principal part of the integral.

Expression (9a) is characteristic for the resonant interaction of a discrete level with orbitals that have a contineous energyspectrum (10,11). If $\Gamma_i(\alpha_i) \ll |E_{max} - E_{min}|$, E_{max} and E_{min} being the upper and lower bound of the energyspectrum of orbitals ϕ_k, the interaction between adsorbate and surface metal orbitals can be considered weak. Then $\Lambda_i(E)$ and $\Gamma_i(E)$ can be assumed to be energy independent.

Within this approximation the energy distribution of the adsorbate level is Lorentzian. The interaction of the 4σ orbital is representative for this situation. One observes in figure 4 the very small level shift of the 4σ CO orbital compared to the corresponding energy in the non interacting molecule. The distribution is symmetrical around its maximum as predicted by eq. (8). The orbitals below $\alpha_i + \Lambda_i$ are bonding orbitals, the orbitals above $\alpha_i + \Lambda_i$ are antibonding orbitals. The difference in energy between the maximum of the bonding orbital fragments and antibonding orbital fragments is $\sim \Gamma(\alpha_i + \Lambda_i)$. Since bonding as well as antibonding orbital fragments are occupied the overall 4σ-metalsurface interaction will be repulsive. The electron occupancy of the 4σ orbital does not change.

Table 2. Gross population Extended-Hückel of CO adsorbed on Rh surfaces.

orbital	adsorbate	atop			bridge	3-fold	step
		(111)	(100)	(110)	(111)	(111)	(111)
1π	ads.	0.998	0.998	0.998	0.996	0.996	0.932
	free	1.0	1.0	1.0	1.0	1.0	1.0
5σ	ads.	0.884	0.882	0.895	0.873	0.873	0.840
	free	1.0	1.0	1.0	1.0	1.0	1.0
$2\pi^*$	ads.	0.136	0.125	0.135	0.228[1)]	0.261	0.368
	free	0.0	0.0	0.0	0.0	0.0	0.0

1): average value of $2\pi^*$ orbitals with (occupation of 0.278) and with π_y (0.178) symmetry.

As is shown in table 2 this is different for the CO 5σ and $2\pi^*$ orbitals. As follows from figures 1 and 2 the relative position of these orbitals with respect to the Fermi level are such that upon interaction the antibonding 5σ-surface metal orbital fragments are pushed above the Fermi level, resulting in a depletion of 5σ electron occupancy. The bonding $2\pi^*$-surface metal orbital fragments are pulled below the Fermi level. Figures 5 and 6 show the corresponding local densities of states. Wheres in the atop position the 5σ LDOS remains nearly symmetrical, a broadening towards higher energies is seen in higher coordination sites. The deviation from the Lorentzian line shape is larger for the $2\pi^*$ LDOS. It implies that the weak adsorption assumption according to which the energy dependence of $\Lambda_i(E)$ and $\Gamma_i(E)$ is ignored is not valid any more. Using the definition of the surface metal grouporbital density (5,6), (9a) can be rewritten as:

$$\Gamma_i(E) = \pi \sum_g |\langle \varphi_i | H' | \phi_g \rangle|^2 \, \rho_g^m(E) \qquad (10)$$

The energy dependence of $\Gamma(E)$ is related to the metal metal surface group orbital local density of states, that interacts with adsorbate orbitals φ_i. For a transition metal the group orbitals ϕ_g can be considered as a particular linear combination of d, s and p valence atomic orbitals of the same symmetry as orbital φ_i. $\rho_g^m(E)$ has only a finite value as long as $E_{max}^g > E > E_{min}^g$. The boundaries of the energy spectrum of each metal surface group orbital are not necessarily the same. The d-valence electron

orbitals have a relatively narrow bandwidth, whereas the s, p valence electron band is very broad. For a metal lattice with one s-atomic orbital per metal atom $\rho_g^m(E)$ has the general form:

$$\rho_g^m(E) = \frac{1}{\sqrt{\overline{n}}\,|\beta|}\, f_g^m(E) \tag{11}$$

$\overline{n}$ is the number of surface metal atom nearest neighbour metalatoms and β the overlap energy integral between two metal nearest neighbour atoms. With (7) and (11), $\Gamma_i(E)$ can written in the normalized form:

$$\Gamma_i(E) = \pi \sum_j \frac{n_{ij}\beta'^2_{ij}}{\sqrt{\overline{n}_j}|\beta_j|} \cdot f^m_{g(j)}(E) \tag{12a}$$

$$= \pi \sum_j \mu_{ij}\, \sqrt{n_{ij}}\, \beta'_{ij}\, f^m_{g(j)}(E) \tag{12b}$$

μ_{ij} is a measure of the interaction strength.

$$\mu_{ij} = \frac{\sqrt{n_{ij}}\,\beta'_{ij}}{\sqrt{\overline{n}_j}\,\beta_j} \tag{12c}$$

With (12b), expression (8) is rewritten as:

$$\rho_i(E) = \frac{\sum_j \mu_{ij}\,\sqrt{n_{ij}}|\beta'_{ij}|f^m_{g(j)}(E)}{(\alpha_i + \wedge_i(E) - E)^2 + \left[\sum_j \mu_{ij}\sqrt{n_{ij}}\,\beta'_{ij} f^m_{g(j)}(E)\right]^2} \tag{13}$$

We will analyse the general behaviour of (13) as a function of coupling parameter μ_{ij}, restricting ourselves initially to the case of one adsorbate orbital and a metal lattice consisting of one s-atomic orbital per metal atom. The general behaviour of (13) is sketched in figure 7. $\rho_i(E)$ is expected to have in general several maxima. One maximum corresponds to the value of E, that satisfies:

$$\alpha_i + \wedge_i(E) - E = 0 \tag{14}$$

Its solution is given by $\overline{\alpha}_i$, the upwards or downwards shifted adsorbate level. The direction of the shift depends whether it corresponds to a bonding or antibonding orbital fragment of the interacting system. In figure (7) it has been chosen to be a bonding level. The other maxima derive from $f^m_{g(j)}(E)$. In figure 7 it has been assumed that the valence electron band has one maximum. For a general discussion we refer to (3). When $\mu \ll 1$, ρ_i is Lorentzian around $\overline{\alpha}_i$ with half width $2\Gamma_i(\overline{\alpha}_i)$. With increasing μ the energy distribution becomes asymmetric and a second maximum at $\overline{\alpha}_m$ appears. At a small value of μ, the weak chemisorption limit fragment orbital levels below $\overline{\alpha}_i$ are bonding and above $\overline{\alpha}_i$ are antibonding. We recognize in figures 5 and 6 the increasing asymmetry and the appearance of a separate antibonding and antibonding density when the coordinationnumber with the surface metal atoms increases. As discussed in the previous section the bond strength contribution to the adsorbate-surface chemical bond depends on the distribution of the electrons over bonding and antibonding adsorbate metalsurface fragment orbitals. In formal chemisorption theory the expression for the covalent contribution to the bond strength is given by (4,9):

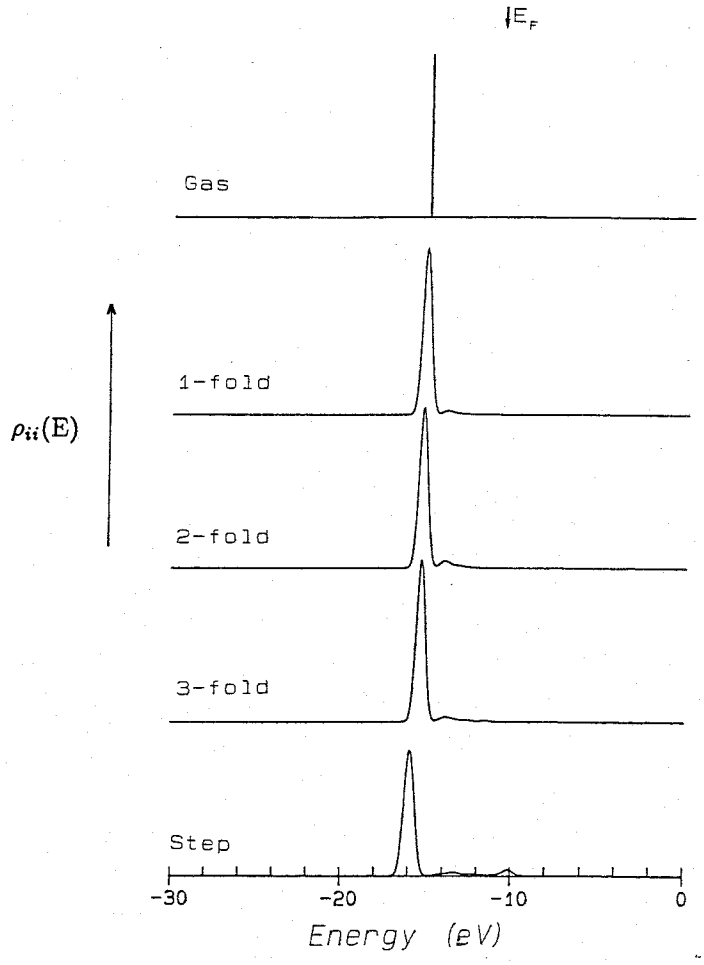

Figure 4

LDOS of the 1π CO molecular orbital in the gas phase, of CO atop adsorbed on Rh (111), of CO 2-fold adsorbed on Rh (111), 3-fold adsorbed on Rh (111) (distance of CO to step 1.551Å). The Fermi level is indicated by E_F.

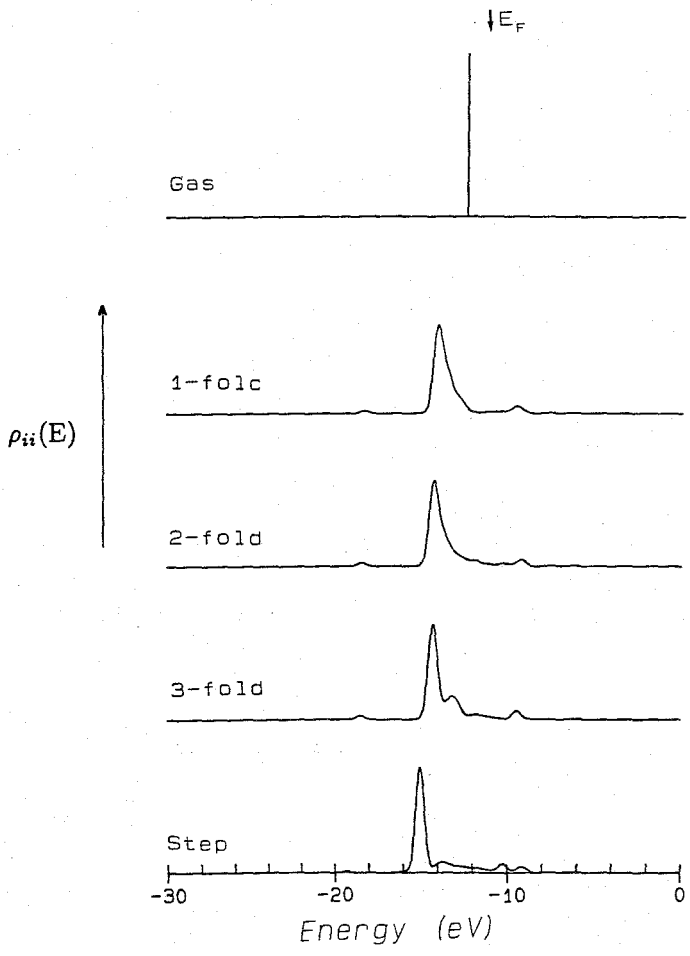

Figure 5

LDOS of the 5σ CO molecular orbital in the gas phase of CO atop adsorbed on Rh (111), of CO 2-fold adsorbed on Rh (111), 3-fold adsorbed on Rh (111) and 3-fold adsorbed on stepped Rh (111) (distance of CO to step 1.551Å). The Fermi level is indicated by E_F.

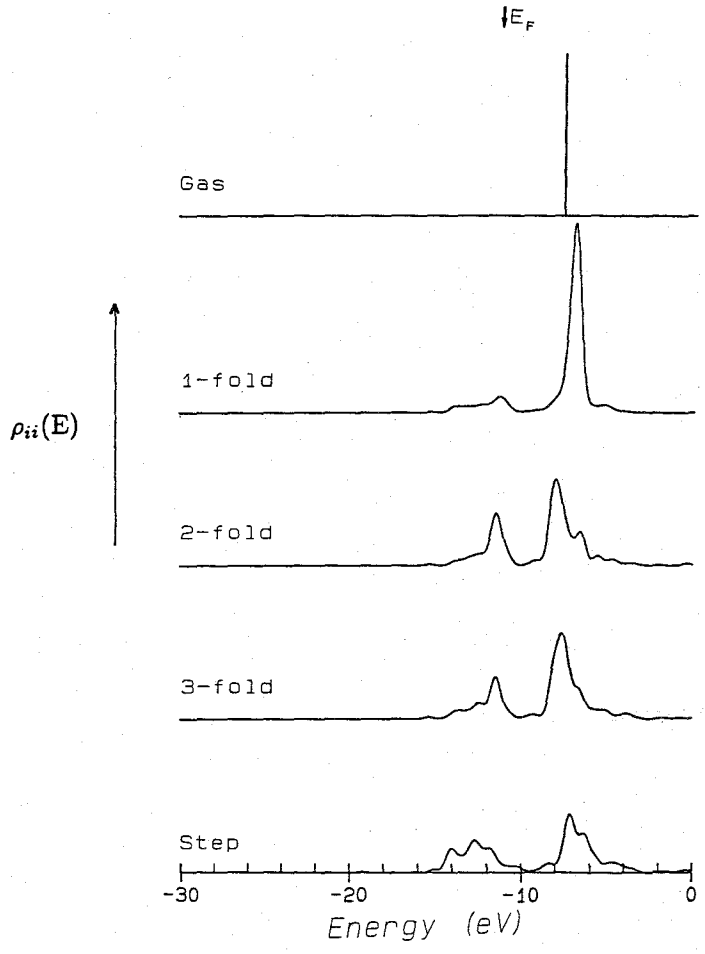

Figure 6

LDOS's if the $2\pi^*$ CO orbitals in the gas phase of CO atop adsorbed on Rh (111), of CO atop adsorbed on Rh (111), of CO 2-fold adsorbed on Rh (111), 3-fold adsorbed on Rh (111) and 3-fold adsorbed on stepped Rh (111) distance of CO to step 1.551Å). The Fermi level is indicated by E_F.

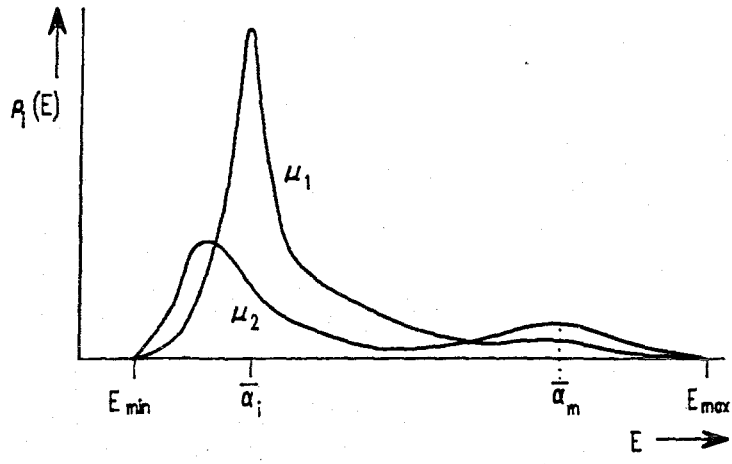

Figure 7

$\rho_i(E)$ as a function of μ (schematic),$\mu_2 > \mu_1$.

$$\Delta E_i = \frac{2}{\pi} \int_{-\infty}^{E_F} dE \eta_i(E) \tag{15a}$$

$$\operatorname{tg} \eta_i(E) = \frac{\Gamma_i(E)}{\alpha_i + \Lambda_i(E) - E} \tag{16a}$$

$\eta_i(E)$ can be considered the phaseshift of the surface electrons scattered by the adsorbate. For weak adsorption the behaviour of $\eta_i(E)$ is sketched in figure 8.

One recognizes that at values of $E < \overline{\alpha}_i$ there is bonding contribution to the energy, but at energy values above $\overline{\alpha}_i$ the contribution is antibonding.
In the weak adsorption limit, the attractive covalent contribution to the bond energy is approximately given by:

$$\Delta^w_{cov} = \frac{2}{\pi} \int_{-\infty}^{E_F} dE \frac{(\overline{\alpha}_i - E)\Gamma}{(\overline{\alpha}_i - E)^2 + \Gamma^2} \tag{17a}$$

$$\approx \frac{2\Gamma(E_F)}{\pi} \ln \frac{(\overline{\alpha}_i - \overline{E}_F)^2 + \Gamma^2(E_F)}{(\overline{\alpha}_i - E_{min})^2} \tag{17b}$$

Remember that $\Gamma(E_{min}) = \Gamma(E_{max}) = 0$. Note that $\ln \left| \frac{(\overline{\alpha}_i - E_F)^2 + \Gamma^2}{(\overline{\alpha}_i - E_{min})^2} \right|$ is minimum when $E_F = \overline{\alpha}_i$. At this value of E_F all bonding orbitals are filled. At a higher value of E_F the bond energy decreases because antibonding levels become occupied. $\Gamma(E_F)$ follows from (12):

$$\Gamma(E) = \pi n \beta'^2 \rho^s_g(E) \tag{18a}$$

$$= \frac{\pi n \beta'^2}{\sqrt{\overline{n}} |\beta'|} f^m_g(E) \tag{18b}$$

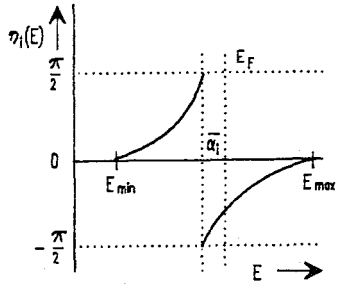

Figure 8

The phaseshift $\eta(E)$ as a function of energy.

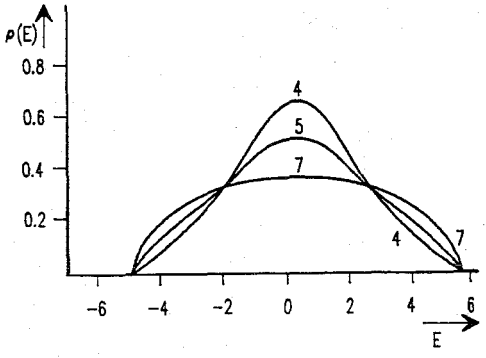

Figure 9

LDOS of a surface atom in the Bethe lattice approximation. Numbers denote the number of surface atom neighbour atoms. Bulk coordination is 8.

As mentioned earlier the linewidth function $\Gamma(E)$ relates with the corresponding metal surface grouporbital local density of states. In the general case the local density of states contains significant structure. Its approximate behaviour is sketched in figure 9 (the density is correct up to its second moment). The width of the surface local density of states is proportional to $\sqrt{\overline{n}}$, $\overline{n}$ is the number of metalatom neighbours of a surface atom. Because $\rho^s(E)$ is normalized the maximum of $\rho^s(E = E_{max})$ is inverse proportional to $\sqrt{\overline{n}}$:

$$\rho^s(E_{max}) \sim \overline{n}^{-1/2} \tag{19}$$

As long as E_F is not close to the edges of $\rho^s(E)$:

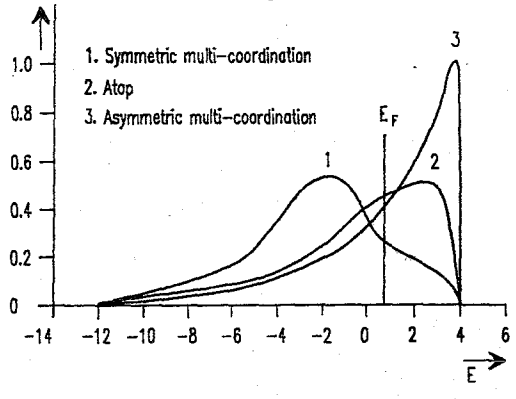

Figure 10

Metal surface group orbital local densities of states (schematic).

$$\Delta_{cov} \approx -\frac{\pi\, n\, \beta'^2}{\sqrt{\bar{n}}\,|\beta|} \tag{20}$$

Expression (20) is expected to hold when an adsorbate interacts with a valence electron band that is half filled. The attractive contribution to the covalent energy is lowest on surface atoms with a high degree of coordinative saturation. It increases when the degree of coordinative saturation of the surface atomes increases. When the energy dependence of $\rho_g(E)$ is ignored, the bond strength increases with adsorbate coordination-number. As sketched in figure 10 the maximum density of a group-orbital corresponding to a symmetric combination of atomic orbitals is lower than the LDOS of an individual atomic orbital and that of an asymmetric combination of atomic orbitals is higher than the LDOS of an individual atomic orbital (11). This affects the bonding part to the bond energy ΔE^w_{cov}, because according to (17b) it relates to $\Gamma(E_F)$. In the weak adsorption-limit according to (18a) ΔE^w_{cov} depends on the grouporbital local density of states at the Fermi level. Therefore dependent on Fermi level position the relative stability of coordination of adsorption sites changes. In agreement with the discussion in section 2, a high valence electron band occupation favours atop adsorption for σ-symmetry adsorbate orbitals, but a low valence electron band occupation threefold coordination. The group VIII transition metal Pt has a nearly completely filled d-valence electron band. We argued in section 2 that changes of the interaction of the CO 5σ, and the surface metal d orbitals dominate coordination of CO to Pt. The analysis presented here not only agrees with this, it also predicts that CO binds most strongly atop to the (111) surface (7). Only at lower d-valence electron occupation coordination to the more open surfaces becomes favoured.

Elsewhere (6) we demonstrated that the perpendicular threefold coordination of O_2 to the (111) surface of silver optimizes the interaction of the occupied O_2 1π orbital with the asymmetric group orbital local density of states around the Fermi level. It was also shown that bonding of O_2 to the silver surface is only well understood if not only the interaction with the s,p valence electron band density close to the Fermi level, but also formation of bonding and antibonding orbital fragments with d-valence electrons is

included. The narrow d-valence electron band and the many d-valence atomic orbitals results in a high LDOS of completely filled orbitals. They interact significantly with the partially occupied π-valence orbitals of O_2. This interaction turns out to be repulsive when O_2 is adsorbed parallel but attractive when O_2 is adsorbed perpendicular to the (111) surface.
According to formal chemisorption theory the attractive contribution to the covalent energy is found to be the sum of two terms:

$$\Delta E^{at}_{cov} = 2\sum_{i,j} n_{ij}\,\beta'^{\,2}_{ij}\,\overline{\rho^{s}_{g(j)}\,(E_F)}\,\ln\left\{\frac{(\overline{\alpha}_i - E_F)^2 + \Gamma^2_{ij}(E_F)}{(\overline{\alpha}_i - E^j_{min})^2}\right\}$$

$$- 2\sum_{j}\frac{n_{ij}\mid\langle\varphi_i\mid H'\mid\varphi_{dj}\rangle\mid^2}{E_F - E_{dj}} \qquad (21a)$$

The last term has to be included if adsorption to a IB metal is studied. Expression (21a) has to be applied with care to a transition metal with d-valence electron holes. The expression for $\overline{\rho^{s}_{g(j)}}(E_F)$ to be used is $\rho^{s}_{g(j)}(E_F)$ averaged over an energy interval in the order of $\Gamma(E_F)$.
Expression (21a) shows explicidly the interesting result that in the limit of weak adsorption, there exist a relation between the group orbital local density of states at the Fermi level and chemisorption energy. In the derivation of (21a) adsorbate and surface molecular orbitals have been assumed to be orthogonal.We have analysed the consequences of non-orthogonality extensively elsewhere (3). The form of expressions (21a) does not essentially change. However an additional repulsive interaction is now introduced. We have shown (3) and already discussed shortly in section 2 that the repulsive interaction equals:

$$E_{rep} = 4\sum_{i,k}^{occ}\langle\varphi_i\mid H'\mid\phi^m_k\rangle\mid\langle\phi^m_k\mid\varphi_i\rangle$$

$$\approx 4\sum_{k}^{occ}\sum_{i,j}\left\{n_{ij}\,\beta'_{ij}\,S_{ji}\,q^k_{g(j)}\right\} \qquad (21b)$$

Since $\beta'_{ij} \sim S_{ij}$, the repulsive part to the bond energy is proportional to S^2_{ij}

$$\approx 4\sum_{i,j} n_{ij}\mid S_{ij}\mid^2 q_{g(j)}\,(E_F) \qquad (21c)$$

with:

$$q_{g(j)}\,(E_F) = \int_{-\infty}^{E_F} dE\,\rho_{g(j)}\,(E) \qquad (22)$$

$q_{g(j)}(EF)$ is the electron occupation of surface group orbital $\phi_{g(j)}$.

Applications to metal promotion

GENERAL BACKGROUND

Coadsorption of adatoms or alloying may change the nature of the adsorbate-metal surface chemical bond for steric as well as electronic reasons. The ensemble effect (12) is used to explain changes in bond energy due to surface dilution or rearrangement effects. As discussed earlier atoms from an adsorbing molecule will in general bind to several surface atoms. If one blocks surface atoms by coadsorption with inert atoms,

or by alloying with non-reactive elements, the average ensemble size of the surface atoms decreases and hence the probability for adsorption to high coordination sites also decreases. This has been extensively discussed elsèwhere (12). Here we will be concerned with changes in chemical bonding due the consequences of differences in composition on atompositions in the second coordination sphere with respect adsorbate atoms (see fig.11).

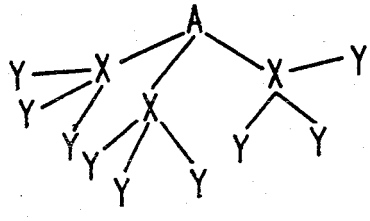

Figure 11

Surface ligand effect. The bond strength between A and atoms on positions X varies due to changes in composition on positions Y.

This may be called surface ligand effect and can be due to changes in covalent bonding or electrostatic effects, resulting from alloying or coadsorption. Changes in surface topology may also be the cause of a surface ligand effect. Several different ways to categorize metal promoters have been proposed. The most natural seems to be to distinguish between electronegative and electropositive coadsorbates or elements (13). Whereas not incorrect, it appears that the overall effect of promoters may differ dependent on the relative position of promoting atom and adsorbate. We will discuss this specifically for the electropositive promoting elements. Here we will distinguish electronic changes in surface chemical bonding due to the presence of promotors according to whether they affect the repulsive or attractive part of the potential energy curve of the adsorbate-surface chemical bond. In the weak adsorption limit the expression for the attractive and repulsive part of the potential energy curve are given by (21a) and (21c). The attractive part of the potential energy is mainly determined by the grouporbital local energy density of states at the Fermi level or the relative position of the adsorbate orbitals with respect to the surface Fermi level position. The repulsive part of the potential energy curve stems from Pauli-repulsion between doubly occupied orbitals. It depends on the overlap of adsorbate and metal surface wavefunctions as well as the occupation of the surface grouporbital interacting with adsorbate. Due to the presence of a promotor the spatial distribution of the surface-electrons may change, resulting in a change in overlap of adsorbate and surface wavefunctions. Also the orbital electron occupation may change. The latter may result in a change in the electron distribution over bonding and antibonding orbital fragments. We will discuss an example where the promoting atom reduces the occupation of antibonding orbital fragments, so that a repulsive interaction is changed into an attractive one.

Note that the attractive contribution to the bond strength depends on the group orbital local density of states at the Fermi level, but that the repulsive part of the potential energy curve depends on the total electron occupation of the surface grouporbitals. Usually several changes in the bonding parameters occur when a promoting atom or ion coadsorbs. We will discuss a few examples that illustrate the usefulness of an interpretation of promotoreffects in terms of changes of the attractive and repulsive part of the bond strength potential energy curve. Sulphur and alkali coadsorption are examples where the attractive part of the adsorbate-surface metal potential energy

curve changes. Metal particles adsorbed to cations, situations that occur on catalyst supports or in zeolites may show reduced Pauli-repulsion. The enhanced reactivity of oxygenations adsorbed to the silversurface in the presence of subsurgace oxygen or chlorine resulting in selective ethylene epoxidation is an example where a repulsive interaction is changed in to an attractive one (8). The electronic basis to the reduction of reactive ensemble atoms size by alloying with an insert element is the Pauli repulsion between adsorbate and insert atom.

Changes of the attractive part of the potential energy curve

Experimental studies on the effect of S, C or P adsorption on CO adsorption show (14) that the rate of CO adsorption is significantly more affected by the presence of these adsorbates than can be explained on the basis of geometric constraints due to a decrease of the effective reactive surface atom ensemble size. Feibelman e.a. (15) computed the variation in electron density on a surface due to the presence of coadsorbed S. As reproduced in figure 12 they find that the total electron density only changes on the transition-metalatom that coordinates with sulfur. The local density of states at the Fermi level is significantly changed also on atoms that are not coordinated to S! This applied to expression (21a) for the bond energy explains the reduced interaction with CO. Electron-energy density fluctuations mainly of the s,p-valence electrons are induced by adsorption of S to a transition metal. They depend on the kind of coadsorbate. This has been studied by Joyner e.a. (16).

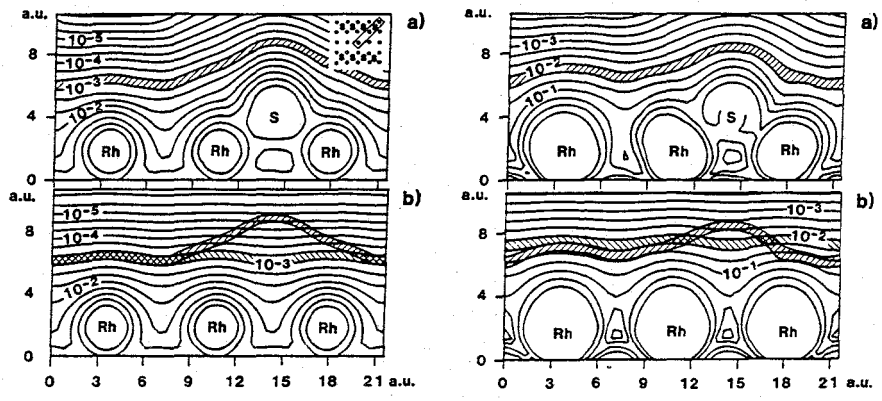

Figure 12

(a) Valence charge densities (in atomic units) for two-layer Rh (001) films (a) with and (b) without a S (3 x 1) adlayer. To facilitate comparison the region between contours of charge density $\sim 10^3$ a.u., about 4 a.u. above the Rh nuclei has been hatched. The hatched region from the S/Rh plot has been transcribed onto that for clean Rh[15].
(b) Fermi level LDOS, in (eV x a^3)$^{-1}$ for two-layer Rh (001) films (a) with and (b) without a S (3x1) adlayer. Regions of equal LDOS have been hatched in the two plots. For comparison the hatched region has been transcribed from the upper to the lower plot[15].

Coadsorption of alkali atoms affects the surface-chemical bond for very different reasons. When an alkali atom adsorbs at low concentration onto a transition metal surface it will develop a small positive charge (N.1e). This is because the difference in alkali-ionization potential and transition metal workfunction is larger than their covalent interaction. The positive adatom charge will be screened by the transition-metal electrons, so that a small negative charge appears on the atoms to which the alkali atom is adsorbed. For a molecule adsorbed close to the alkali atom the result

will be a lowering of the adsorbate orbitals with respect to the metal Fermi level. The dipole generated by the adsorbed alkali atom will lower the workfunction. In (21a) this changes the value of $(\overline{\alpha}_i - E_F)$ to $(\overline{\alpha}'_i - E_F)$. $\overline{\alpha}'_i - \overline{\alpha}_i$ is the potential an electron in absorbate orbital i experiences due to the electrostatic potential generated by the screened alkali atom charge. The results of calculation by Freeman e.a (17). for CO adsorbed to Ni illustrate this nicely (fig. 14).
As follows from equation (21a) two cases can be distinguished.

Case a: $\overline{\alpha}_i > E_F$. This is the contribution to the bond energy due to "electron backdonation". Metal surface orbitals interact with the unoccupied adsorbate orbitals α_i. Because the attractive potential of alkali lowers the adsorbate orbital levels with respect to E_F:

$$\overline{\alpha}'_i - E_F < \alpha - E_F$$

and the contribution to the adsorbate bond strength increases.

Case b: $\overline{\alpha}_j < E_F$. This is the contribution to the bond energy due to "electron donation". Unoccupied metalsurface orbitals interact with occupied adsorbate orbitals α_j . The lowering of the adsorbate orbital levels with respect to E_F gives relation:

$$E_F - \overline{\alpha}_j < E_F - \overline{\alpha}'_j$$

The corresponding contribution to the adsorbate bond energy decreases.

Table 3. Bond energy values of CO adsorbed on Pt.

		top	bridge	top	bridge
val. bands.	mol. orb.	no K		K	
s	5σ	−0.439	−0.293	−0.385	−0.184
	$2\pi^*$		−0.256		−0.474
d	5σ	−0.454	−0.263	−0.241	−0.154
	$2\pi^*$	−0.444	−0.492	−0.531	−0.628
ΔE		−1.337	−1.304	−1.157	−1.440

Bond energy contributions and total Bond energy ΔE (eV) of CO adsorbed to (111) face of platinum. Effect of alkali coadsorption.

$$\begin{aligned}
\alpha_{5\sigma}(K) &= \alpha_{5\sigma} + \Delta V_{\mathrm{CO}} \\
\alpha_{2\pi^*}(K) &= \alpha_{2\pi^*} + \Delta V_{\mathrm{CO}} \\
\alpha_{\mathrm{Pt}_{s,d^s}}(K) &= \alpha_{\mathrm{Pt}_{s,d}} + \Delta V_{\mathrm{Pt}^s} \\
\Delta V_{\mathrm{CO}} &= -0.5eV
\end{aligned}$$

In table 3 results of tightbinding calculations of CO adsorbed to the (111) surface of Pt are presented. A comparison of the relative energies of atop and three-fold coordinated CO is given in the presence and absence of coadsorbed potassium atoms. The presence

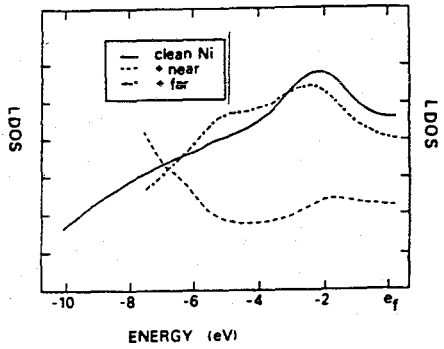

Figure 13

LDOS change on Nickel atom next nearest to adsorbed S atom[16].

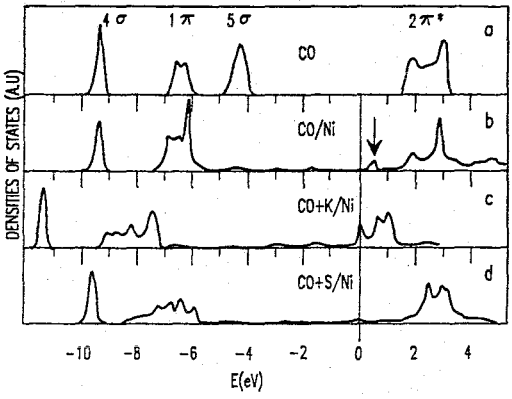

Figure 14

Local density of states of CO adsorbed to Ni[17].
(a) unsupported CO film; (b) CO / Ni
(c) (CO+K) / Ni; (d) (CO+S) / Ni.

of potassium is simulated by a lowering of the CO adsorbate levels with respect to the Fermi level as indicated in table 3. As predicted the interaction with the $2\pi^*$ orbital of CO (backdonation) is found to increase and that with the 5σ orbital of CO (donation) decreases. The overall result is a change in coordination of CO from the atop position to three fold coordination. Especially when the interaction with the s-valence electron band dominates electron backdonation favours high coordination because in order to interact with the metalsurface the CO $2\pi^*$ orbital requires antisymmetric surface metal grouporbitals fragments are occupied. When the interaction with the highly occupied d-valence electron bond is important the donative contribution of σ symmetry favours atop coordination. In the atop configuration the repulsion due to the occupation of antibonding orbital-fragments is minimized (7).

Changes of the repulsive part of the potential energy curve

On a metal surface an alkali-ion will adsorb on the same relative position with respect to the metal surface as the adsorbate. This may be different when one considers small metal particles. In figure 15a we show a configuration where a Mg^{2+} ion is located at the other site of a metal particle than an adsorbed CO molecule. Such a situation may arise in zeolites or metal particles distributed on a MgO carrier. The difference in electron distribution of an Ir_4 particle comparing a situation with no Mg^{2+} ion present and one with a Mg^{2+} ion is shown in figure 15b. The computed result is from a Hartree-Fock-Slater-LCAO calculation (19).

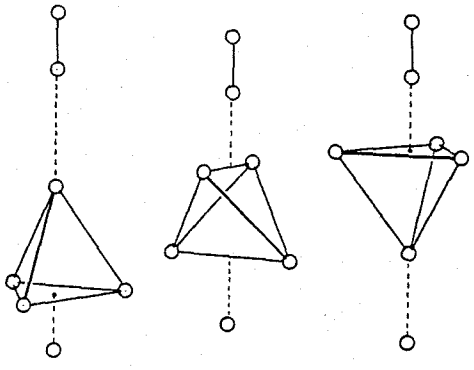

Figure 15a

Relative position of Mg^{2+} and adsorbed CO on a Ir_4 particle.

One observes polarization of the Ir_4 particle. Electron density is pulled towards the Mg^{2+} ion, in order to screen its charge. As a results there is a decrease of electron density on the atom to which adsorbed CO is attached. Table 4 shows a comparison of the Pauli repulsion computed for CO adsorbed atop, twofold or threefold with the Mg^{2+} ion present or absent on the opposite adsorption site of the tetrahedral Ir_4 particle (14). One observes a significant decrease in Pauli-repulsion. The reduction in electron density between CO and neighbouring Ir atoms reduces the Pauli-repulsion between doubly occupied CO-5σ orbitals and occupied Ir_4 orbitals, since according to (21c) Pauli repulsion reduces, when orbital overlap is decreased. The overall result on the CO adsorption strength is no change in adsorbate bond energy, because not only the repulsive part to the bond energy but also the attractive contribution, due to electron backdonation into the CO $2\pi^*$ orbital changes.

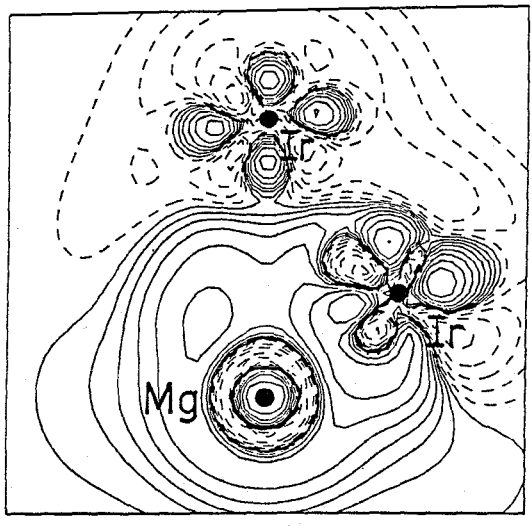

Figure 15b

Change in electron density on Ir_4 cluster close to a Mg^{2+} ion[19].
- - - - - - loss in density
— — — — gain in density.

Table 4a

Adsorption energies and their decomposition (in eV) of CO on a tetrahedral Ir_4 cluster and a Mg^{2+} ion at the opposite side.

geometry	adsorption energy	steric repulsion	interaction energy
1-fold	0.98	0.18	1.16
2-fold	2.35	5.62	7.93
3-fold	2.42	4.78	7.19

Table 4b

Change in the adsorption energies of CO and their decomposition (in eV) upon introduction of the Mg^{2+} ion. Shown are the values with minus values without the cation.

geometry	adsorption energy	steric repulsion	interaction energy
1-fold	0.05	−1.53	−1.48
2-fold	−0.07	−1.86	−1.96
3-fold	0.03	−3.16	−3.11

The CO molecule has a larger distance with respect to the Mg^{2+} ion than the Ir_4 particle. The electrostatic field of the Mg^{2+} ion lowers the Ir_4 electron orbitals more than those of the adsorbate electron orbitals. The result is an increase in the CO $2\pi^*$ orbital energy with respect to the Ir_4 HOMO orbital energy and the electron backdonation contribution decreases. So the loss in repulsion is compensated for by a loss in attraction.

The presence of the cation is only reflected in an increase of the CO stretch frequency due to the decrease in the CO $2\pi^*$ orbital occupancy. Studies of H_2 adsorption show a similar decrease in repulsion interaction as observed for CO, but now overall an increase of the interaction energy is found (20). It may explain the enhanced activity in hydrocarbon conversion activity of metal particles close to positively charged cations in zeolites (21). Significant H_2 bond weakening is found.

The last two examples to discuss derive also from metal catalysis. First we will discuss the electronic basis of the role of subsurface oxygen or chlorine in ethylene epoxidation and we wish to conclude by explaining that the electronic basis to the secondary ensemble effect consists in essence of Pauli-repulsion between adsorbate atoms and inert surface-atoms. Experimental studies of the selectivitiy of ethylene epoxidation catalysed by silver have shown that the epoxidation activity is enhanced by the presence of subsurface oxygen atoms close to the adsorbed oxygen atom to be inserted into the ethylene π bond (22). HFS-LCAO calculations on small silver metal particles demonstrate the reason for this (8). We will present results for 4 silver atom clusters. Whereas details are slightly different, on larger particles the essential physics does not change. A silver atom cluster has been chosen such that atoms are located as on the Ag (110) surface. The different cluster compositions are shown in figures 16. Figure 16a en 16b show an adsorbed oxygen atom in the presence and the absence of subsurface oxygen. Figures 16c and 16d show the configuration studied with ethylene present. The results of the calculation are best analysed by computation of Bond-Order Overlap Population Densities (BOOPD's) (see eq. 2a). Figures 17a and 17b show the BOOPD's of the adatom O-Ag cluster-atoms in the absence and presence of subsurface oxygen. A positive value means a bonding contribution to the bond energy and a negative value an antibonding contribution. E_F denotes the highest occupied molecular orbital. One observes that the adatom O-Ag cluster bond is weakened by the presence of subsurface oxygen. When subsurface oxygen atoms are present antibonding O-Ag orbital fragments become occupied. It results from the reduced difference in energy between the bonding and antibonding O-Ag orbital fragments. The coupling parameter μ (eq. 12c) decreases because Ag has effectively an increased number of neighbours. This reduces the Ag local density of states around the Fermi level of the cluster in fig. 16b. The bond weakening of the oxygen-silver bond due to subsurface oxygen has a very large effect on the interaction with ethylene. The corresponding BOOPD's are shown in figures 18a and 18b. The stronger silver-oxygen bond results in a repulsive interaction with ethylene when no subsurface oxygen is present. This changes in the presence of subsurface oxygen. One observes the depopulation of the antibonding silver-oxygen orbital fragment. The weaker oxygen-silver bond results in a stronger interaction with ethylene and a larger difference in energy between bonding and antibonding oxygen-carbon orbital-fragments.

The concepts discussed can also be used to provide an electronic basis to the concept of ensemble effects in alloy catalysis. Soma-Nota and Sachtler (23) explained the shift of chemisorbed CO from bridging to atop coordination comparing adsorption to Pd with a Pd-Ag alloy to a secoundary ensemble effect. CO interacts weakly with Ag. Alloying with silver does not change the s-p valence electron band very much, but the interaction with d-valence electrons changes significantly. The average energy of the d-valence atomic orbitals on silver is lower than that of the Pd d-valence atomic orbitals. In addition on the Ag atom the d-atomic orbitals are completely occupied. If in a high coordination site a Pd atom becomes substituted by an Ag atom, the interaction with the CO $2\pi^*$ orbitals as well as the 5σ orbitals changes. Backdonation into the CO $2\pi^*$ orbital is reduced because of the larger difference in energy between the CO $2\pi^*$ orbital and part of the d-valence orbitals. Pauli repulsion increases. The CO 5σ orbital now interacts with atoms with doubly occupied d-atomic orbitals giving a repulsive

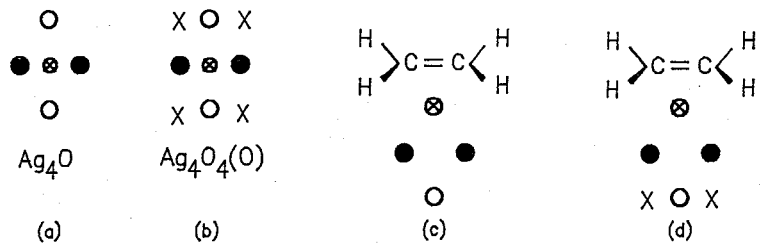

Figure 16

The silver clusters studied; ⊗ chemisorbed oxygen, • silveratom in outerlayer, O silveratom in inner layer, x subsurface oxygen atom;
(a and b) top view without ethylene; (c and d) side view with ethylene[8].

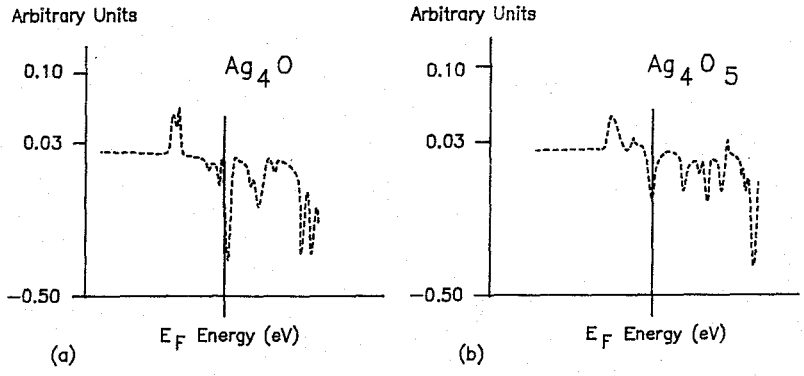

Figure 17

Bond-order overlap population densities of bond Ag-O_{ads};
(a) AgO, (b) Ag_4O_4 (O_{ads})[8].

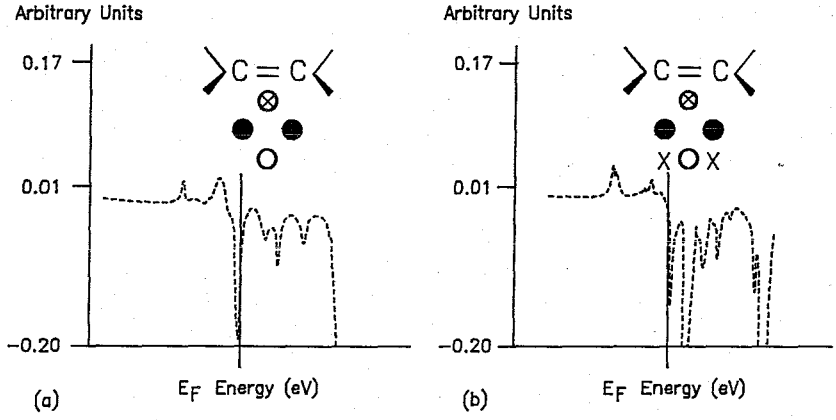

Figure 18

Bond-order overlap densities of ethylene C and O_{ads} orbitals;
(a) without subsurface oxygen, (b) with subsurface oxygen[8].

interaction. Both changes favour preferential adsorption with a site consisting of only Pd-atoms. This will result in a lower coordination number of CO. The importance of the repulsive interaction of the CO 5σ orbitals with doubly occupied orbitals of group IB metals becomes especially apparent from the preferred atop coordination of CO to Cu. This low workfunction metal should have an increased backdonating interaction with the high coordination directing CO $2\pi^*$ orbitals. CO, however, is found to prefer the atopposition. The low average energy of the d-valence electrons is unfavourable to the backdonating interaction and results in a repulsive interaction with the CO 5σ orbital (5).

References

1. G. Blijholder, J. Phys.Chem. 68, 2772 (1064).
2. K. Fukui, Science 218, 747 (1982);
   R.B. Woodward, R. Hoffmann, Ang.Chem.Int.Ed.Engl. 8, 781 (1969);
   Th.A. Albright, J.K. Burdett, M.H. Whangbo, Orbital interactions in chemistry, J. Wiley & Sons (1985).
3. R.A. van Santen, E.J. Baerends, in "Theoretical Models of Chemical Bonding", part. 4, Z.B. Maksic (ed.) Springer Verlag, in press.
4. P.M. Newns, Phys.Rev. 178, 1123 (1969); P.W. Anderson, Phys.Rev. 124, 41 (1964); J.R. Schrieffer, in "Dynamic Aspects of Surf. Physics" (8.0 Goodman, ed). Proc. Int. School of Physics "Enrico Fermi", Course XVII (Ed. Comp. Bologna, 1974);
   T.B. Grimley, CRC Crit.Rev. Solid State Sci. 239 (1976).
5. R.A. van Santen, J. Mol. Struct. 173, 157 (1988).
6. M.C. Zonnevylle, R. Hoffmann, P.J. van der Hoek, R.A. van Santen, Surf.Sci. 223, 233 (1989).
7. A. de Koster, A.P.J. Jansen, R.A. van Santen, J.J.C. Geerlings, Far. Disc. Chem. Soc. 87, 263 (1989);
   A. de Koster, R.A. van Santen, Surf.Sci. 233, 366 (1990).
8. P.J.M. van den Hoek, E.J. Baerends, R.A. van Santen, J. Phys.Chem. 93, 6469 (1989).
9. R.A. van Santen, J. Chem.Soc. Far. Trans. I 83, 1915 (1987).
10. A. Messiah, Quantum Mechanics II, North-Holland Publ.Co, Amsterdam, 1969.
11. R.A. van Santen, Physica 62, 51 (1972).
12. W.M.H. Sachtler, R.A. van Santen, Adv. Catal. 26, 69 (1977).
13. L. Ya Margolis, Adv. Catal 14, 429 (1963).
14. D.W. Goodman, Acc. Chem. Res. 17, 194 (1984).
15. P.J. Feibelman, D.R. Hamann, Phys. Rev. Lett. 52, 61 (1984).
16. J.M. Maclaren, J.B. Pendry, R.W. Joyner, P. Mechan, Surf.Sci. 175, 263 (1986); J.M. Maclaren, J.B. Maclaren, J.B. Pendry, R.W. Joyner, Surf.Sci. 178, 856 (1986).
17. E. Wimmer, C.L. Fu, A.J. Freeman, Phys.Rev.Lett. 55, 2618 (1985).
18. R.A. van Santen, Proc. 8th Int. Congr. on Catal., vol IV, Springer-Verlag, Berlin, 1984, p. 97.
19. A.P.J. Jansen, R.A. van Santen, J. Phys. Chem. in press.
20. E. Sanchez-Marcos, A.P.J. Jansen, R.A. van Santen, Chem. Phys. Lett. 167, 399 (1990).
21. P. Gallezot, Catal. Rev.-Sci Eng. 20, 121 (1979).
22. R.A. van Santen, H.P.C.E. Kuipers, Adv. Catal. 35, 265 (1987).
23. Y. Soma-Nota, W.M.H. Sachtler, J. Catal. 32, 315 (1974); Y. Soma-Nota, W.M.H. Sachtler, J. Catal. 34, 162 (1974).